

MEMS for the masses part 2: comparison to geophones in field data

Michael S. Hons, Robert R. Stewart, Don C. Lawton and Malcolm B. Bertram

ABSTRACT

Field data from Violet Grove, Alberta are examined to determine under what conditions data acquired through geophones and MEMS is materially different, which is to say under what conditions they do not perform exactly as their response characteristics predict. Both sensors perform very much as expected down to very small excitation magnitudes. Within the smallest amplitudes in the field data, the lower noise floor of the MEMS sensors may be apparent at very high frequencies. The greatest differences between the sensors appear at large amplitudes (i.e. large ground motion). The MEMS appears to record lower amplitudes immediately above the dominant frequencies, and lower amplitudes above 95 Hz. Simple processing applied to the field gathers might demonstrate greater coherence in the MEMS data amongst high frequencies, but results on whether this represents a reflection event is inconclusive.

INTRODUCTION

It has been established in part 1 that geophones are expected to have a flat amplitude response to velocity above its mechanical resonance, with a second order drop in amplitudes at frequencies below resonance. The phase spectrum changes from -180° at very low frequencies (below $1/10$ of resonance) to 0° at very high frequencies (above $10 \times$ resonance). Response curves can be described as being in reference to velocity or acceleration domain. The particular mix of amplitudes and phase lags output from a geophone does not represent any ground motion domain, even approximately, and might be best labeled as 'geophone domain'. MEMS accelerometers are expected to have a flat amplitude response and a zero phase response to acceleration, and thus their output can be considered to be 'acceleration domain'. However, as long as each sensor performs precisely along this expected response, correcting amplitudes and phase lags to be comparable to each other, or to represent any ground motion domain (including acceleration) is as simple as applying the inverse of the appropriate frequency response. If there were no nonlinearities or differences in noise floor between the sensors, there would be no material difference in the data acquired. Part 1 also described how (at present) the geophone should have a noise floor advantage over the MEMS at frequencies near the geophone's resonance, but a higher noise floor at frequencies above ~ 50 Hz. The noise floor below 10 Hz will quickly become dominated by $1/f$ noise, and both sensors will likely encounter noise problems at similar signal amplitudes and frequencies. The recording noise floor will only be apparent where it is not overwhelmed by ambient noise.

This paper presents field data from a sensor test near Violet Grove, Alberta. The sensor test consisted of 225 shots recorded into 8 stations, as described by Lawton et al., 2006. At each station two 3C geophones and one 3C Sercel DSU were planted; at two of the stations a third 3C geophone was also present. Each of the sensors was planted one

meter apart. Examination of the receiver records will hope to establish whether significant differences were found under field conditions.

FIELD DATA

The field data were recorded during a monitor VSP survey at a CO₂ injection site. There were 8 stations, with a station interval of 20 m. Each station was occupied by two geophones (ION Spike and OYO Geospace 3C) and one MEMS unit (Sercel DSU3); two stations also had a third geophone (OYO Geospace Nail). All geophones elements had a 10 Hz resonant frequency and 0.7 damping ratio. A photograph of the three geophones and an example cutaway of a DSU3 are shown in Figure 1 (Lawton et al., 2006). A photograph of a station with the DSU, ION Spike and OYO Nail is Figure 2.

The sensors were spaced apart by ~1 m, and comparisons between the geophones should be able to identify how much variability is due to differences between sensor locations rather than sensor element characteristics. In particular, the ION Spike and OYO Nail are very similar in construction, with all three components housed within a casing that is completely driven into the ground. Variability between them should be indicative of the differences due to sensor offset. The OYO 3C sensor, on the other hand, relies on a long thin spike extending from the center of the case, and an auxiliary spike near the edge of the case for coupling. The geophone elements remain above the ground surface.

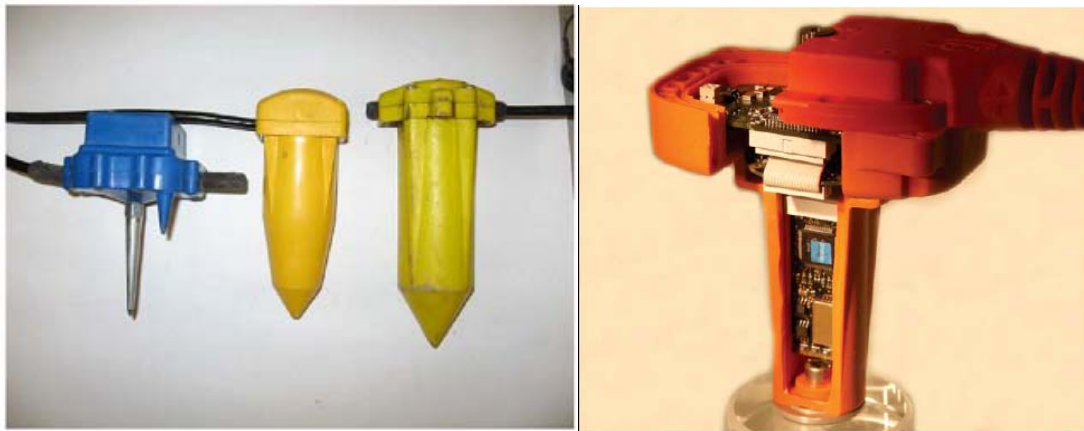


FIG. 1. Geophones used in the sensor test. From left to right: OYO Geospace 3C, ION Spike, OYO Geospace Nail (Lawton et al., 2005), Sercel DSU3.



FIG. 2. From the top: OYO 3C (blue), ION Spike (orange) and DSU3 (red) (Lawton et al., 2005).

There were a total of 225 shots recorded, 75 shots each on 3 lines (Figure 3). The data considered here is a receiver gather from station 5183 (on the north end of the 8 stations), recording shots from line 1 (the N-S trending line). This is one of the stations that was occupied by all three geophones as well as the MEMS accelerometer. This gather is representative of the broader dataset (Lawton et al., 2006).

A ground acceleration gather was calculated from each geophone gather according to the frequency domain correction derived in Part 1 of this paper. All comparisons in this paper will compare the acceleration receiver gathers to the raw MEMS data. The choice to calculate acceleration from the geophones rather than geophone equivalent data from the MEMS accelerometer was made to avoid suggestions that anything has been ‘thrown out’ of the MEMS accelerometer data.

The three geophones recorded extremely similar data, as shown in the time domain (acceleration) in Figure 4. Cross-correlations between corresponding traces from different geophones are generally larger than 0.99. Average amplitude spectra for the gathers are shown in Figure 5. To find the average amplitude spectrum, the amplitude spectrum for each entire trace is calculated, and then the spectra for the traces are averaged without any kind of amplitude balancing. Thus the average spectra are heavily weighted towards traces and times with large amplitudes (middle traces and first breaks). The average spectra show very significant differences between the geophones and the MEMS. In particular just above the dominant frequencies, and at frequencies greater than ~ 95 Hz. The fact that all the geophone spectra are very similar to each other eliminates several possible reasons for the observed differences. Namely, they are not due to the 1 m offset between sensors or local near surface changes, or differences in the cases (either ground coupling or resonance related). This leads to the conclusion the observed differences are inherent to differences within the sensor elements. Two of the most significant differences within the sensor elements are the greater moving mass and larger internal displacement within the geophone. Nonetheless, both sensors have constraints on linear operation, so once differences have been isolated it is difficult to discern which sensor was more directly representative of ground motion.

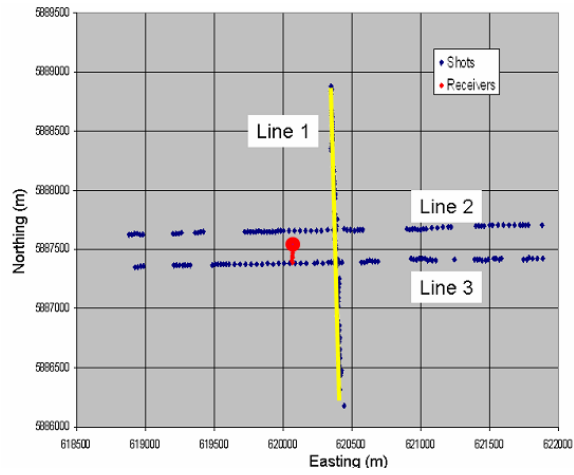


FIG. 3. Base map. Navy are shot locations, red are receiver locations. Line 1 is annotated in yellow and station 5183 is the heavy red dot (after Lawton et al., 2005).

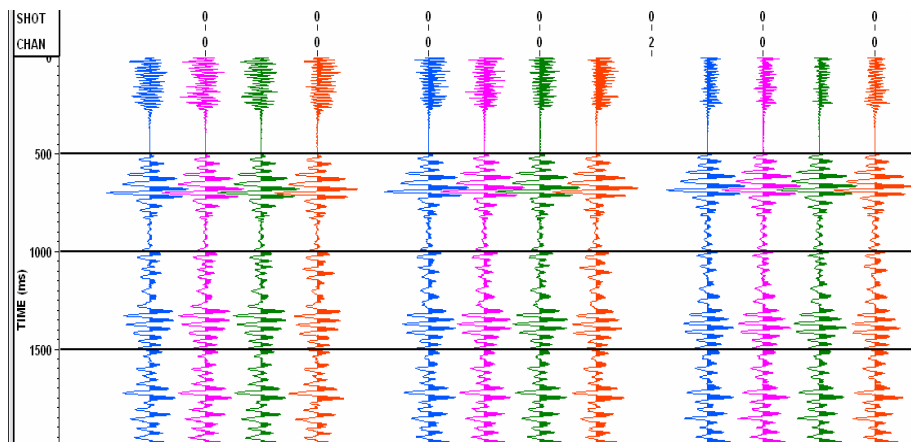


FIG. 4. Trace by trace comparison in acceleration domain: blue is ION Spike, pink is OYO 3C, green is OYO Nail and red is Sercel DSU3. Vertical component data, 500 ms AGC applied.

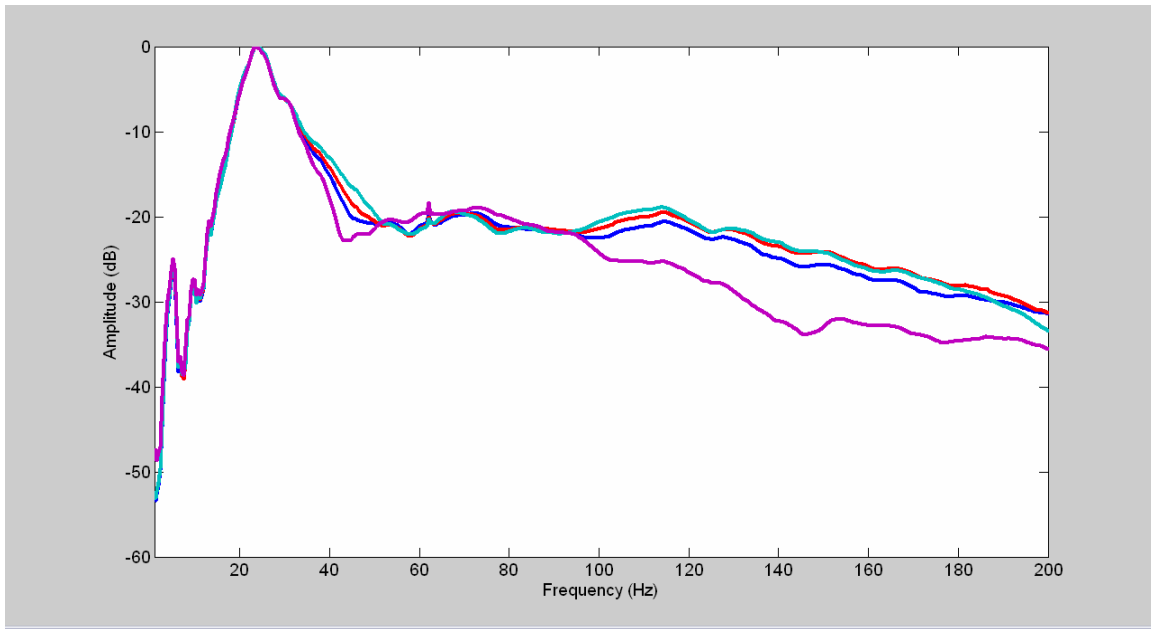


FIG. 5. Average amplitude spectra of the four sensors. Blue is ION Spike, red is OYO 3C, aqua is OYO Nail and purple is Sercel DSU3. Vertical component.

Before examining the reflection data itself any further, the noise floors of the sensors can best be compared by isolating time before the first breaks. In this region, only ambient and recording noise should be present. It provides the opportunity to compare the noise floors of the sensors and whether those noise levels are significant relative to the ambient noise. Figure 6 shows a region of a receiver gather prior to the first breaks, and Figure 7 shows the amplitude spectra of the four sensors. The geophone is expected to have less sensor-related noise above ~50 Hz. The geophone amplitude spectra start to significantly diverge from each other at around 100 Hz, and the below-surface geophones diverge from the MEMS nearer 150 Hz. It is likely that the similarity of the amplitude spectra up to these higher frequencies is due to the ambient noise being much larger than the sensor and channel noise. Indeed, even the discrepancy between the OYO 3C and the other two geophones is likely due to the fact that the OYO 3C sits on top of the earth, while the other two geophones and the DSU house the sensor elements inside the portion that sits below the surface. This leaves the OYO 3C most exposed to wind noise. Also note that there is significant 62 Hz background noise, even in the Sercel DSU data. This is likely due to some mechanical vibration in the ground. It is unlikely that a MEMS sensor could pick up an oscillating magnetic field as strongly as an analog geophone. Also, there is the peculiar trend that the noise becomes stronger as the trace number increases. Recall this is a receiver gather, so power line noise should be of consistent magnitude. A possible explanation is that the dynamite shots are exciting a vibration in some nearby structure, and high mechanical quality of the structure means the oscillation is not damped to its initial state prior to the next detonation. If that structure was related to power transmission, that would explain the unlikely coincidence of the ‘resonance’ being near 60 Hz. In any case, it seems that recording with MEMS accelerometers will not be the end of 60 Hz noise in seismic data.

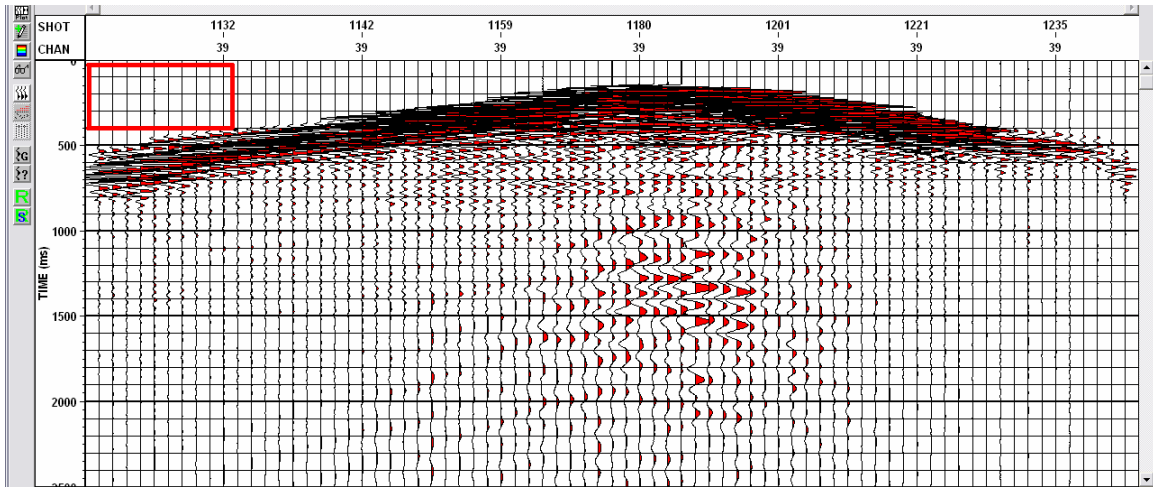


FIG. 6. Example receiver gather, showing area before first breaks.

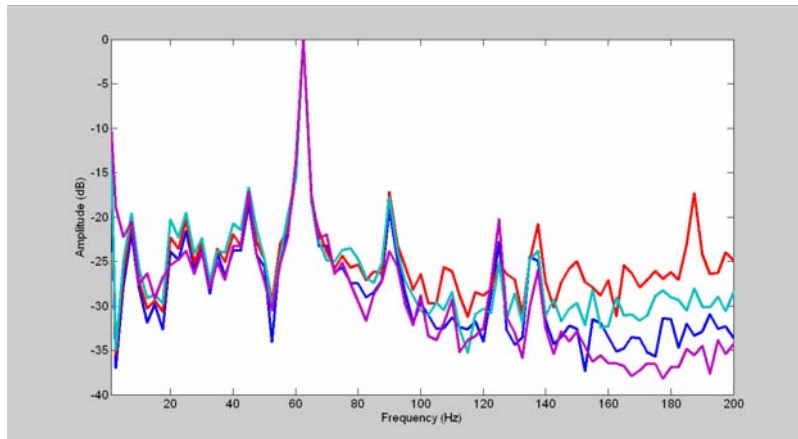


FIG. 7. Amplitude spectra from the four sensors in the area defined above. Blue is ION Spike, red is OYO 3C, aqua is OYO Nail, and purple is Sercel DSU3. Vertical component.

Moving on to the rest of the data, the receiver gather was broken up into 25 sections, shown in Figure 8. Each section contains a 500 ms portion of 15 traces. This was used to sort out which areas of the record most contributed to the differences observed in Figure 5. Figure 9 shows the four spectra (ION Spike, OYO 3C, OYO Nail and Sercel DSU) averaged for windows 5, 10, 15, 20, 25. We can see something very similar to what we saw prior to the first breaks. The OYO 3C, which sits above the ground's surface, splits from the others first, which is interpreted to be due to higher noise. The fact that it splits from the other geophones is likely due to the higher environmental noise (note that the character is generally the same in the other sensors, but the amplitudes are lower). The two geophones below the ground's surface are very near each other over all frequencies, and the DSU has the lowest amplitudes, which is interpreted as an expression of the differences in the noise floors between geophones and MEMS, as discussed in part 1. The significant differences in Figure 5, namely the steeper rolloff after the dominant frequency and the substantially lower amplitudes above ~95 Hz, are not seen in the lowest windows. Figures 10 and 11 show the average spectra across second lowest and middle rows.

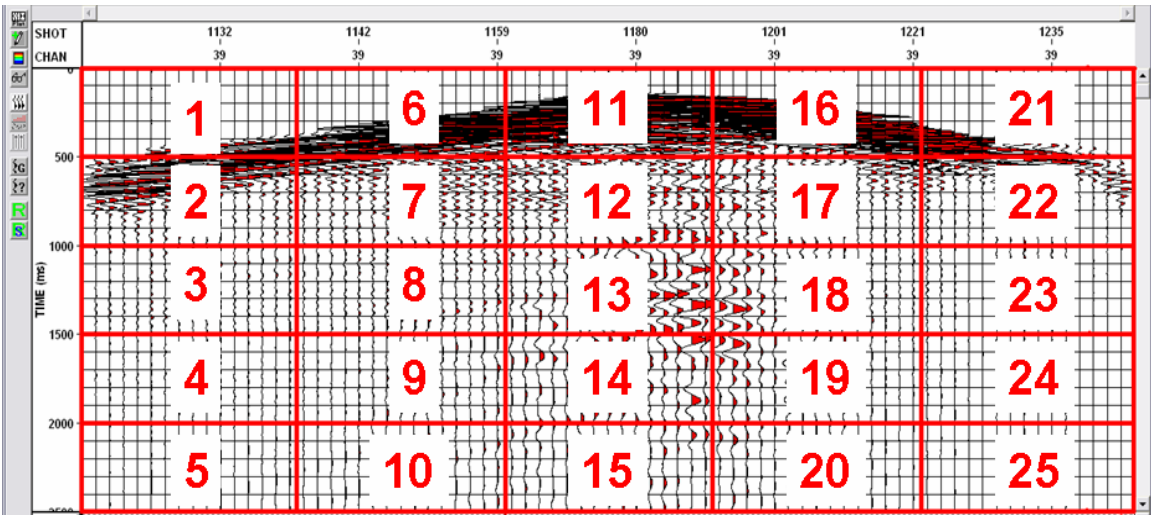


FIG. 8. Receiver gather divided into 25 windows.

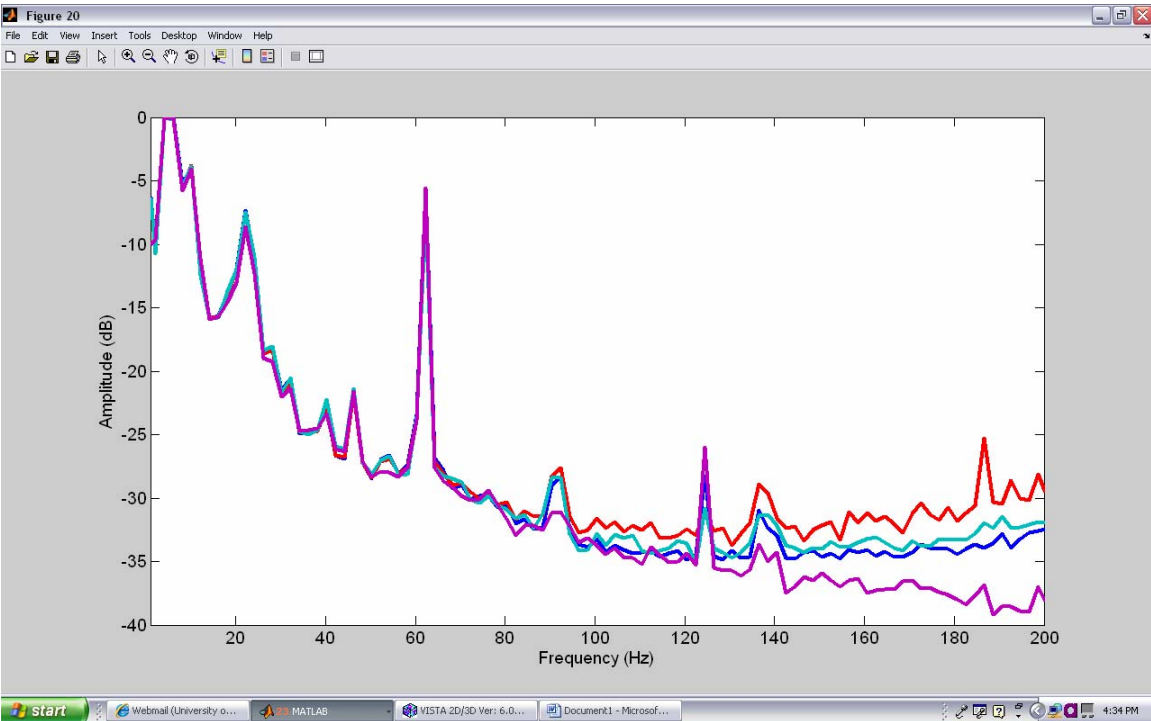


FIG. 9. Average amplitude spectra over windows 5, 10, 15, 20 and 25. Blue is ION Spike, red is OYO 3C, aqua is OYO Nail, and purple is Sercel DSU3. Vertical component.

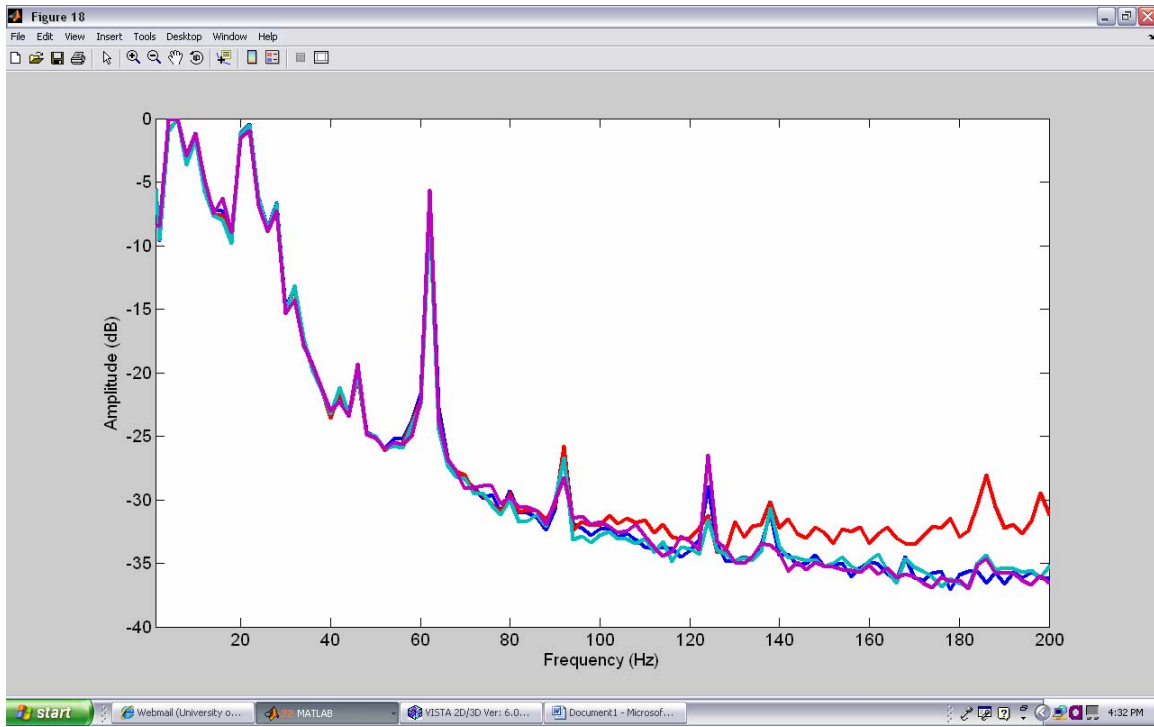


FIG. 10. Average amplitude spectra over windows 4, 9, 14, 19 and 24. Blue is ION Spike, red is OYO 3C, aqua is OYO Nail, and purple is Sercel DSU3. Vertical component.

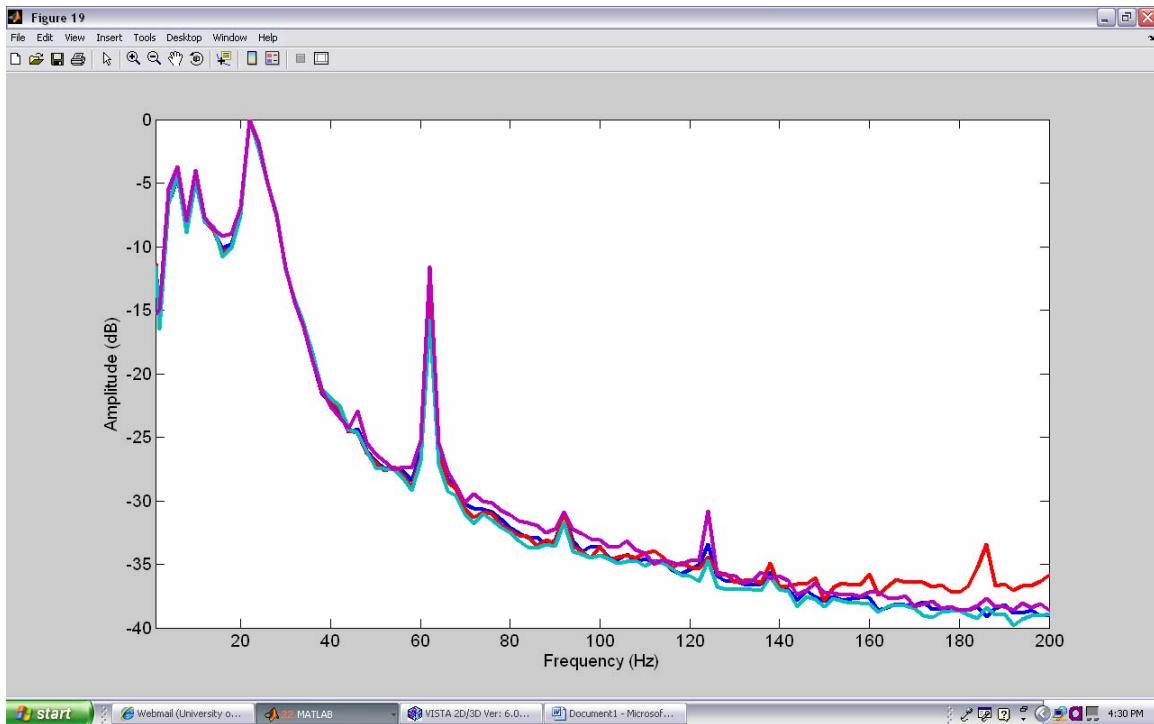


FIG. 11. Average amplitude spectra of windows 3, 8, 13, 18 and 23. Blue is ION Spike, red is OYO 3C, aqua is OYO Nail, and purple is Sercel DSU3. Vertical component.

Clearly the amplitude spectra of the four sensors within these medium scale amplitudes are nearly identical. Apart from some extra high frequency noise picked up on the OYO 3C record, there is no significant difference to the character or magnitude of the recorded spectra. In this intermediate range of amplitudes both sensors performed as expected: each sensor exactly along their expected response, so when both are corrected to the same domain using the responses the spectra are nearly identical. The electrical noise within the recording system is negligible down to 2 seconds, as no significant difference between the MEMS and geophones is observed. The electrical noise at high frequencies must be hidden below some remnant noise related to the shot.

Since the differences in the spectra in Figure 5 have not yet been observed, they must be contained in the upper two rows of windows. This is seen in Figures 12 and 13. In Figure 12 the difference at frequencies >95 Hz is observed, while in Figure 13 the steeper slope just above the dominant frequencies is seen as well. This seems to suggest that moderately high amplitudes result in the differences above 95 Hz, while very large amplitudes are required to produce the differences just above the dominant frequencies. The individual windows with the highest amplitudes most clearly express the differences between the sensors. Window 11 is shown as an example (Figure 14).

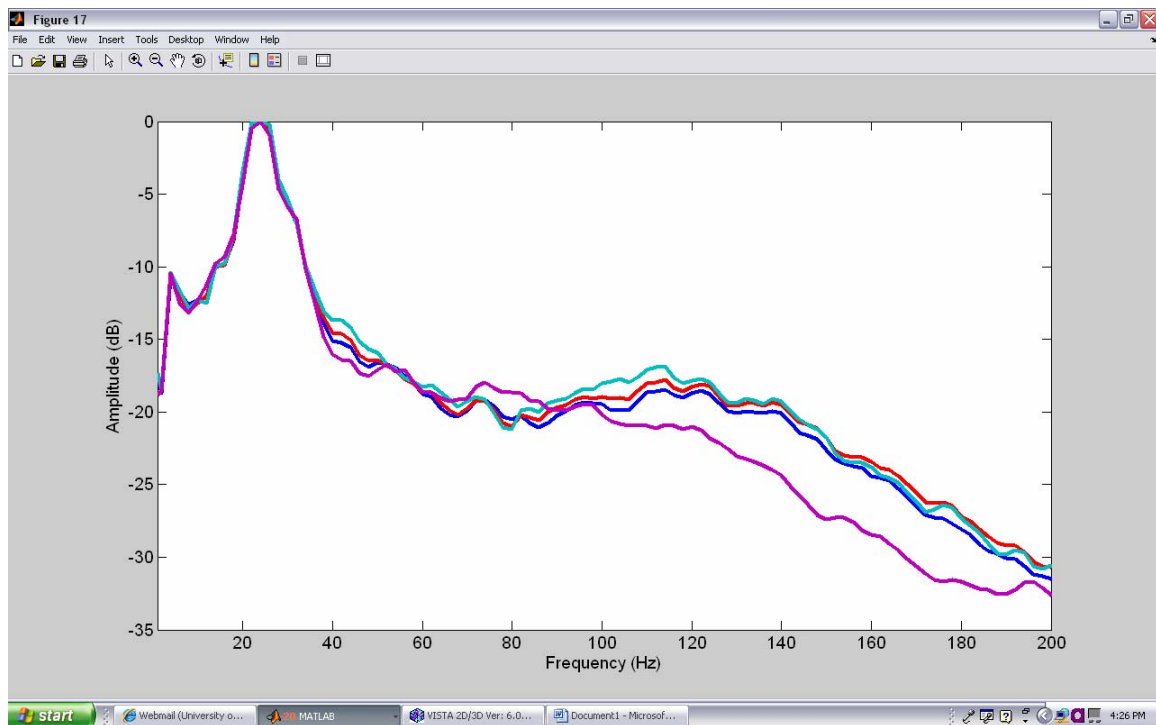


FIG. 12. Average amplitude spectra of windows 2, 7, 12, 17 and 22. Blue is ION Spike, red is OYO 3C, aqua is OYO Nail, and purple is Sercel DSU3. Vertical component.

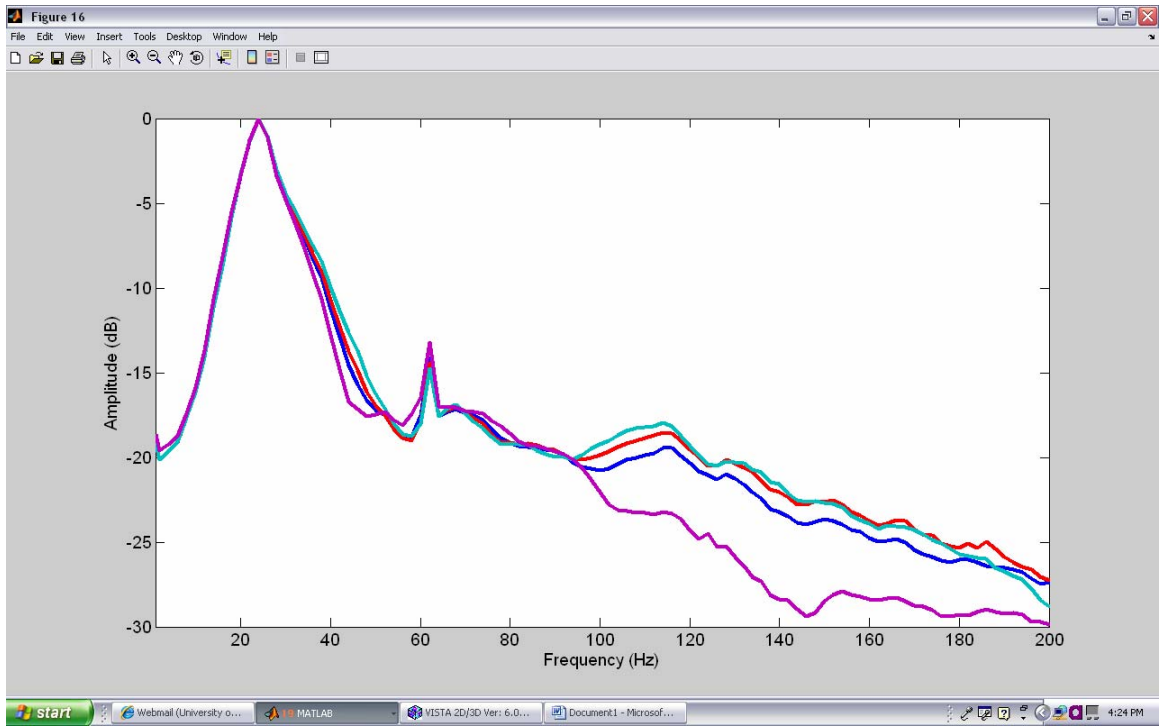


FIG. 13. Average amplitude spectra of windows 1, 6, 11, 16, and 21. Blue is ION Spike, red is OYO 3C, aqua is OYO Nail, and purple is Sercel DSU3. Vertical component.

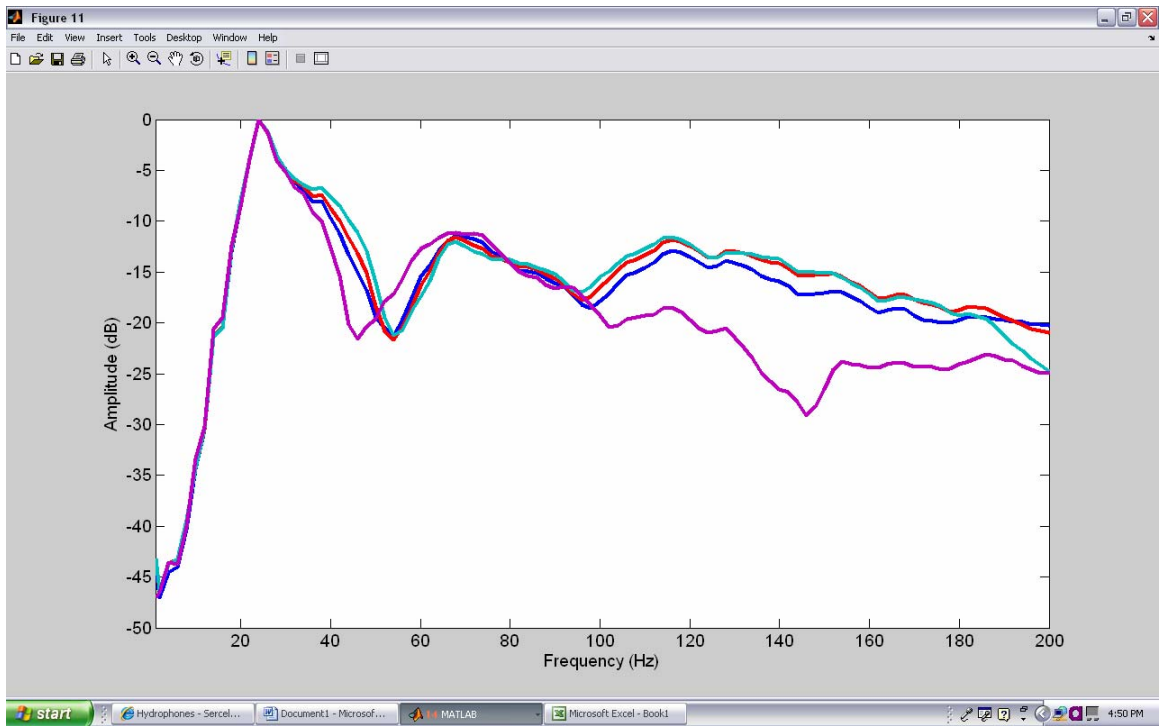


FIG. 14. Average amplitude spectra of window 11. Blue is ION Spike, red is OYO 3C, aqua is OYO Nail, and purple is Sercel DSU3. Vertical component.

Some simple processing was performed to try and help determine whether the larger amplitudes in the geophone gathers represented coherent data. First, elevation statics were applied. Then a semblance plot was created and used to pick NMO velocities. These velocities were applied to the gathers, and a 30% stretch mute was used to remove overly distorted data. The elevation statics and NMO corrected gathers were filtered to frequencies greater than 95 Hz, and those of the OYO Nail and Sercel DSU are shown in Figures 15 and 16. Finally the traces within each gather were stacked, and the amplitude spectrum of each output trace was compared to see what differences remained. Those differences are shown in Figure 17.

Comparing the filtered NMO corrected gathers shows that there is very little apparent signal above 95 Hz. Nonetheless, in the marked area there appears to be more significant energy lining up in the DSU gather (Figure 16) than in the best of the geophone gathers (Figure 15). The DSU appears to be somewhat less noisy at these high frequencies. No lining up of events above 1 second was observed. This is not to suggest that there is no reflection energy in these records above 1 second, just that it is strongly overshadowed by first break energy and shot noise.

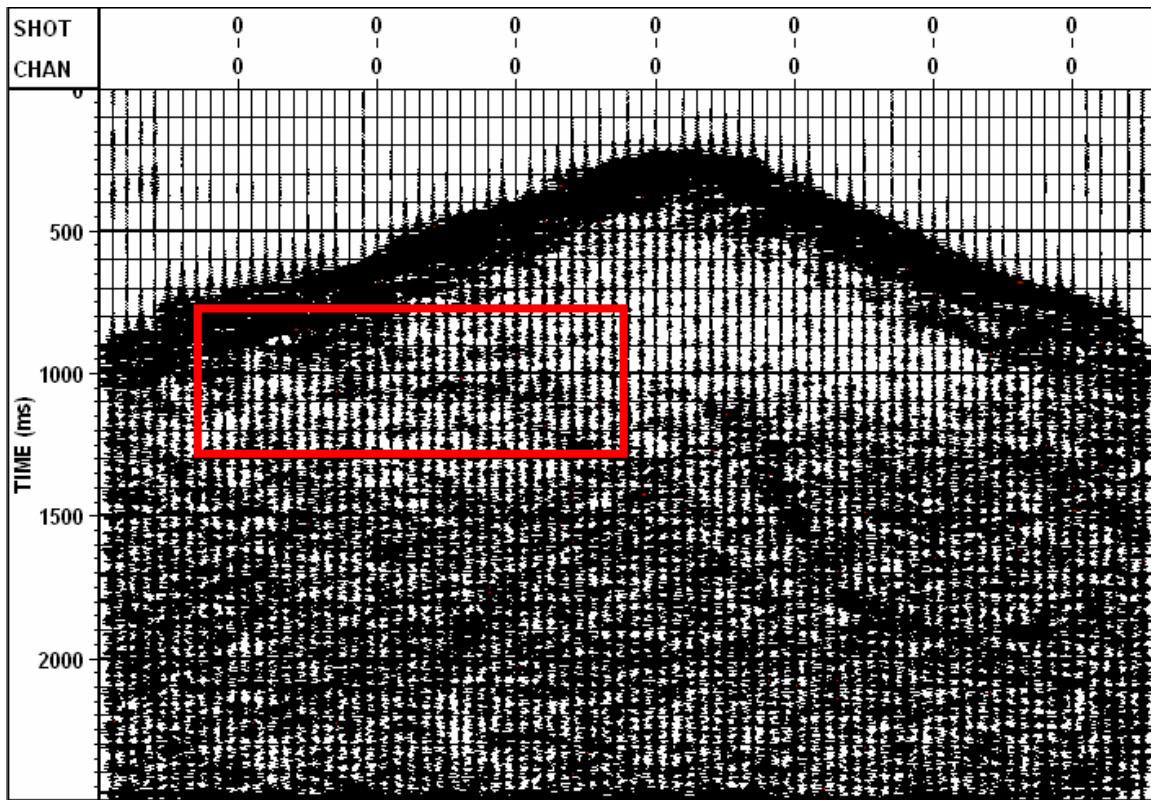


FIG. 15. OYO Nail elevation static and NMO corrected gather, bandpass between 95 and 150 Hz. 500 ms AGC applied.

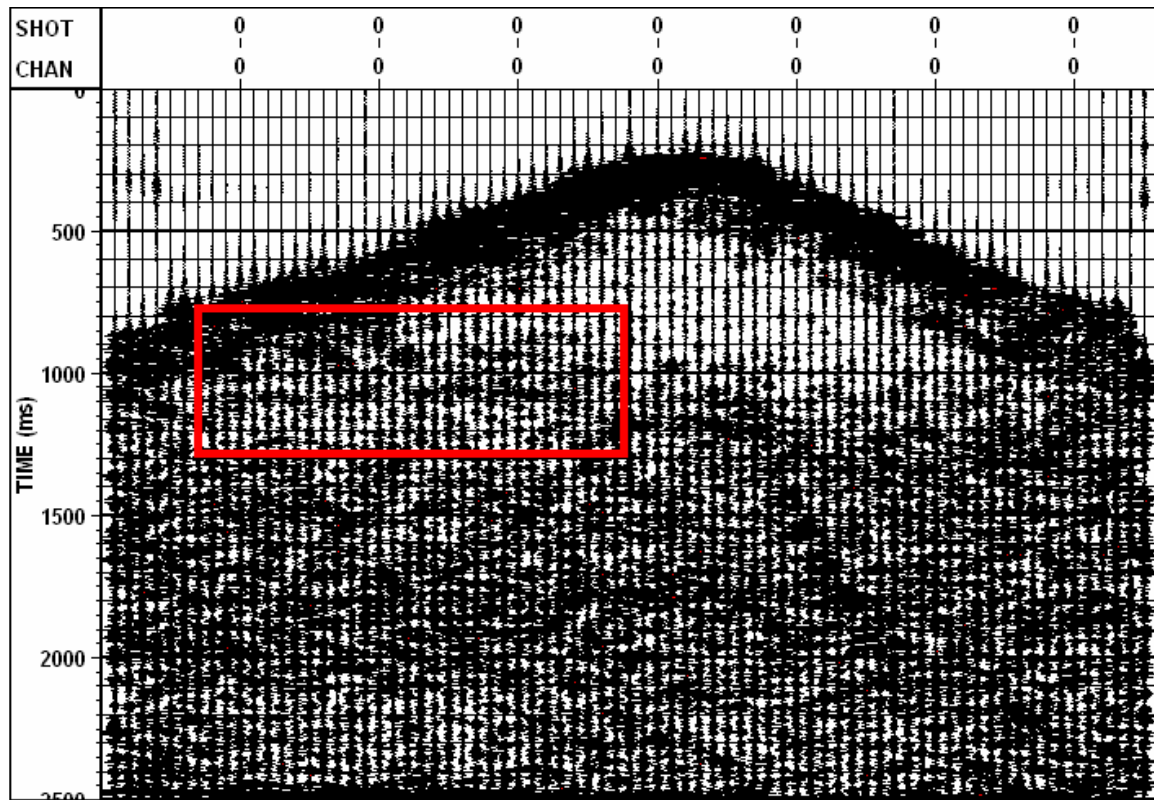


FIG. 16. Sercel DSU elevation static and NMO corrected gather, bandpass between 95 and 150 Hz. 500 ms AGC applied.

Figure 17 shows the four spectra, after each gather has been stacked up to one trace. This stacking relies on the notion that reflections will be very flat and homogeneous. Due to the geological setting, flat reflections are expected, but the consistency and coherency may vary across a record. Also, the trace amplitudes were not scaled relative to each other prior to stacking. This makes the stacked trace highly dependent on the central traces with larger amplitudes, but presumably also stronger reflections. However, this reduces the ability of the stack to remove noise, and may result in noise from the center traces remaining.

Figure 17 shows the high amplitudes between 90 and 120 Hz remain in the geophone data, but the spectra are very similar up to that point. The difference between the sensors just above the dominant frequencies is not retained. In order to improve the ability of the stack to cancel out nonhorizontal events and noise, the elevation static and NMO corrected gathers were also normalized prior to stacking. The spectra for the resulting traces are shown in Figure 18. In this case no significant differences between the sensors are observed.

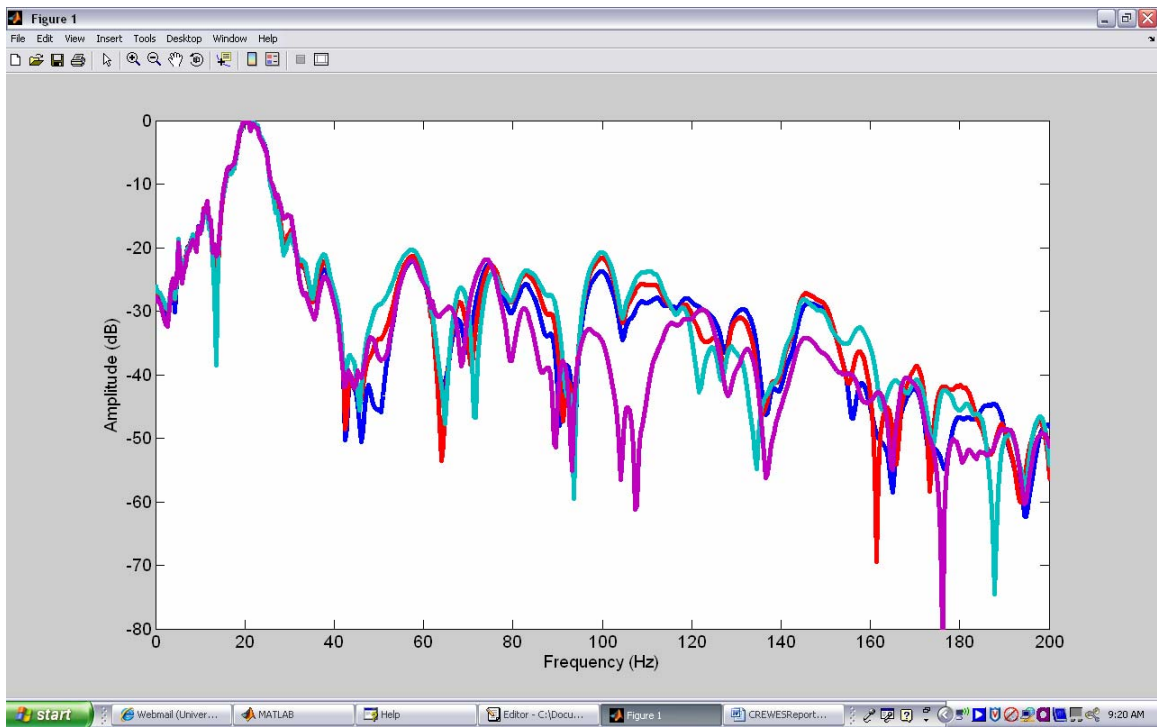


FIG. 17. Spectra of the four stacked traces.

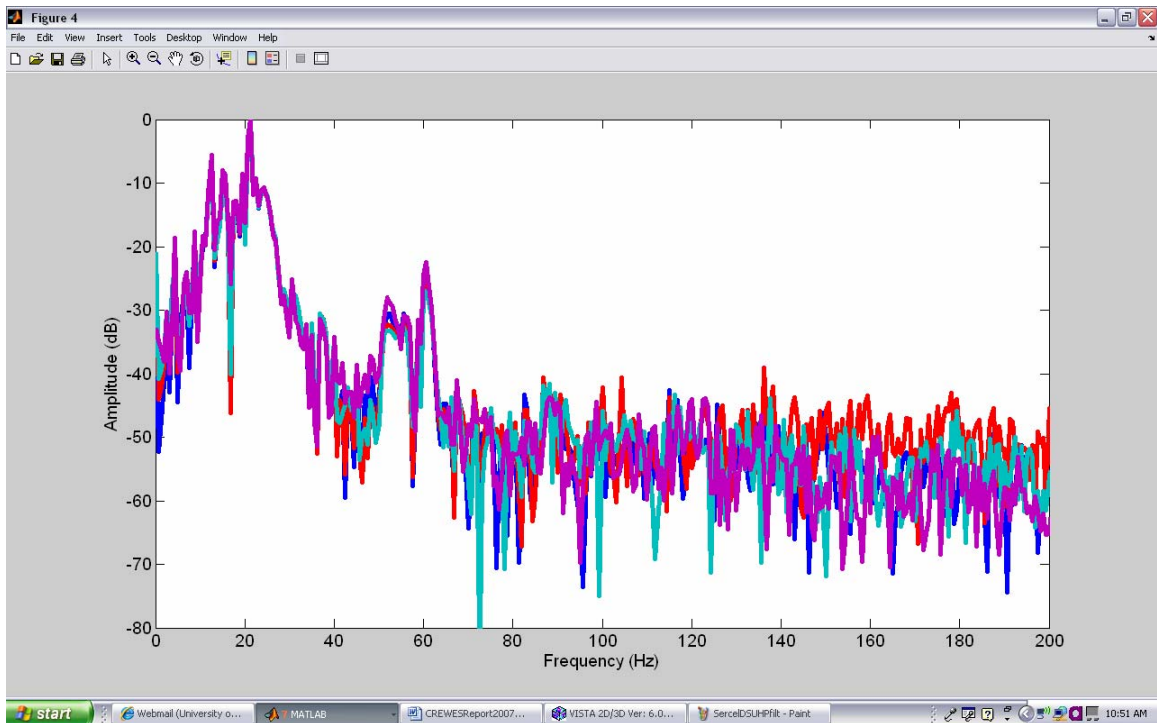


FIG. 18. Spectra of the four stacked traces, with normalization prior to stacking.

CONCLUSIONS

Field data confirms that geophones and MEMS sensors respond as predicted by their respective responses over a range of very small to moderate amplitudes. For very weak signals and high frequencies, MEMS appear to have a noise floor advantage at high frequencies, where the ambient noise is low enough to allow for the difference relative to geophones to be noticeable. This occurs in this dataset at high frequencies (100 to 150 Hz) before first breaks and at greater than 2 seconds travelttime. Large differences are seen only in the case of strong excitation, which means those differences will be removed as the high amplitude shot-related noise events are minimized during processing. The differences are relevant, however, to methods that seek to use the full-wave 3D motion of the ground to separate wave modes, like polarization (Zheng, 1995) and modal filters. Further study is required to determine which sensor more accurately represents the motion of the ground under strong excitation conditions.

ACKNOWLEDGEMENTS

Thanks to Glenn Hauer of ARAM Systems Ltd. and all of the CREWES sponsors.

REFERENCES

- Lawton, D. C., Bertram, M. B., Margrave, G. F. and Gallant, E. V.; 2006; Comparisons between data recorded by several 3-component coil geophones and a MEMS sensor at the Violet Grove monitor seismic survey: CREWES research report, **18**, 2.1-2.24.
- Zheng, Y.; 1995; Seismic Polarization Filtering: Noise Reduction and Off-line Imaging: M. Sc. Thesis, Univ. of Calgary.